Environmental Science and Pollution Research (2022) 29:35138–35149
https://doi.org/10.1007/s11356-022-18721-1

RESEARCH ARTICLE

Viscose-derived activated carbons as adsorbents for malathion, dimethoate, and chlorpyrifos—screening, trends, and analysis

Ana Jocić[1] · Stefan Breitenbach[2,3] · Igor A. Pašti[4] · Christoph Unterweger[2] · Christian Fürst[2] · Tamara Lazarević-Pašti[1]

Received: 25 September 2021 / Accepted: 13 January 2022 / Published online: 19 January 2022

Abstract

The release and accumulation of pesticides in the environment require the development of novel sustainable technologies for their removal. While adsorption is a classical approach, the design of new materials with enhanced adsorption properties could rationalize the remediation routes and decrease potential risks for their non-target organisms, including humans. More importantly, the use of adsorbents and their synthesis should be implemented in a sustainable and environmentally friendly manner. In this contribution, we studied the adsorption of organophosphorus pesticides (OPs) dimethoate, malathion, and chlorpyrifos on viscose fiber–derived activated carbon fibers (ACFs). The most efficient adsorption was found for chlorpyrifos, followed by malathion and dimethoate, while material properties were correlated with OP uptake. These ACFs are extremely efficient for chlorpyrifos adsorption, with experimentally observed adsorption capacitances reaching 240 mg g^{-1}. Detailed analysis suggests that chlorpyrifos is physisorbed on ACF surfaces and that increased surface hydrophilicity reduces the uptake. Studied ACFs have great potential for practical application. They can reduce OPs' concentrations to such levels that no acute neurotoxic effects of the studied OPs in spiked tap water samples are seen, even for starting concentrations up to 10^4 times higher than the allowed ones. Finally, this study presents possible guidance for developing even more efficient and environmentally friendly adsorbents for chlorpyrifos, the most toxic among studied OPs.

Keywords Pesticide removal · Dimethoate · Chlorpyrifos · Malathion · Physisorption · Activated carbon fibers

Introduction

Organophosphorus pesticides (OPs) are a class of chemicals that are considered to be some of the most hazardous but at the same time some of most used today, especially outside the EU and USA (Dehghani et al. 2017; Lazarević-Pašti et al. 2018). OP compounds are the most diverse pesticides available and represent about 40% of total pesticides recorded globally (Dehghani et al. 2017). Due to their impact on a wide range of pests, they play an important role in agricultural production and public health pest control. However, due to their high consumption, they have become a significant source of environmental pollution (Dehghani et al. 2017). The high toxicity of OPs is associated with an irreversible inhibition of the enzyme acetylcholinesterase (AChE), which is vital for normal nerve function in animals, including insects and humans. Moreover, some products of OP chemical transformations and degradation are considerably more toxic than primary pesticides, like their oxidized forms, oxons (Colovic et al. 2013).

Adsorption can be used as an efficient method to remove OPs based on the application of various adsorbents. Carbon materials have found an irreplaceable role in this process, as being rather cheap and having desirable surface properties, like large specific surface area and rich surface chemistry (Uddin 2021). It particularly relates to activated

Responsible Editor: Angeles Blanco

✉ Tamara Lazarević-Pašti
lazarevictlj@yahoo.com; tamara@vin.bg.ac.rs

[1] University of Belgrade, VINČA Institute of Nuclear Sciences - National Institute of the Republic of Serbia, Mike Petrovica Alasa 12-14, 11000 Belgrade, Serbia

[2] Wood K plus –KompetenzzentrumHolz GmbH, Altenberger Strasse 69, 4040 Linz, Austria

[3] Institute of Chemical Technology of Inorganic Materials (TIM), Johannes Kepler University Linz, Altenberger Strasse 69, 4040 Linz, Austria

[4] Faculty of Physical Chemistry, University of Belgrade, Studentski trg 12-16, 11158 Belgrade, Serbia

carbons (ACs), for which specific surface area is greatly enhanced using chemical or physical methods. Such ACs are particularly interesting if derived from waste materials such as biomass (Demirbas 2009). The research in this field is very intense, and some recent reports suggest a successful application of biomass-derived ACs for OP removal, including dimethoate (Ndifreke and Pasaoglulari Aydinlik 2019), malathion (Jusoh et al. 2011), and chlorpyrifos (Yahia et al. 2021; Celso Gonçalves et al. 2021) Among the ACs family, activated carbon fibers (ACFs) have attracted much attention as an adsorbent due to their high surface area, highly developed porosity, and different functional groups, resulting in good adsorption performance (Hassan et al. 2020). These advantageous properties can be tuned by suitable pre-treatments and optimized thermal processing conditions (Breitenbach et al. 2020, 2021). Additionally, using bio-based feedstocks as abundant, available, and low-cost precursors in ACF synthesis makes this adsorbent production sustainable and renewable (Hassan et al. 2020). ACFs' adsorption ability has been demonstrated for various pesticides (Martin-Gullon and Font 2001; Cougnaud et al. 2005; Vukčević et al. 2015) present in water.

In general, adsorption results from the interactions of pesticides with carbon surfaces. So, in addition to the textural characteristics of the adsorbent, the structural properties of adsorbents and adsorbates also play an important role in this process (Lazarević-Pašti et al. 2018). The adsorption mechanisms for OPs are complex since OPs contain different types of functional groups that can interact with the adsorbent (Suo et al. 2018). Therefore, various works have been published addressing the performance and mechanism of adsorption of OPs by different carbon materials. For example, an examination of several pesticides' adsorption on activated carbon monolith (Vukčević et al. 2013) showed that the presence of surface functional groups has a greater effect on adsorption than specific surface areas. In the same work (Vukčević et al. 2013), it was found that the π–π interactions are dominant in the adsorption of pesticides with an aromatic structure. At the same time, acidic groups play an essential role in the adsorption of acyclic pesticides. Similar conclusions are obtained for the adsorption of OPs on graphene-based materials (Lazarević-Pašti et al. 2018). Namely, findings demonstrate that a highly oxidized graphene surface adsorbs only aliphatic pesticide molecules, while a surface with preserved sp^2 hybridization of C atoms adsorbs only pesticides with an aromatic ring. However, a study of chlorpyrifos adsorption on activated carbon also suggested that the interactions are partially chemical and partially physical and mediated via surface functional groups O–H, C–H, C = O, C–C, C–H, and C–O of activated carbon (Celso Gonçalves et al. 2021). Along the same line, the study of OP adsorption on mesoporous carbon material (Lazarević-Pašti et al. 2016) suggested that specific interactions between non-aromatic OP molecules and carbon surfaces exist, mediated by the thiophosphate group. Also, the results obtained for adsorption of several OPs on activated carbon derived from sieve-like cellulose/graphene oxide composites (Suo et al. 2018) suggest that the electron-donating ability of the phosphorus and sulfur atoms generally promotes adsorption.

In this contribution, we investigate and compare the removal of dimethoate (O,O-dimethyl S-[2-(methylamino)-2-oxoethyl] phosphorodithioate), malathion (diethyl 2-[(dimethoxyphosphorothioyl)sulfanyl]butanedioate), and chlorpyrifos (O,O-diethyl O-(3,5,6-trichloropyridin-2-yl) phosphorothioate) from aqueous media using viscose-derived ACFs. To the best of our knowledge, this is the first time that viscose-derived ACFs are used for remediation of the mentioned OPs. Adsorbents' properties are effectively tuned using diammonium hydrogen phosphate (DAHP) as the impregnation agent (Jocic et al. 2021). With a wide range of specific surface area, pore volumes, and tunable chemical composition (C, O, and P), these materials present an excellent basis for analyzing the impact of material properties on pesticide removal. Using a multidisciplinary approach, this work combines adsorption measurements, sets up reliable regression models for the prediction of adsorption efficiency, and rationalizes the presented models using molecular mechanics simulations. Moreover, AChE inhibition, which is a general biomarker for eco-neurotoxicity (Legradi et al. 2018), was also checked and confirmed to be completely alleviated upon treating the OP solutions with studied ACFs. Studied materials have shown excellent performance for chlorpyrifos removal from water, and the ACF-chlorpyrifos interactions are discussed in detail. We find that chlorpyrifos, which contains an aromatic ring, prefers sp^2 hybridized domains of ACFs, pointing to a general strategy for developing highly efficient and eco-friendly adsorbents for chlorpyrifos removal.

Experimental part

Adsorption experiments

The OP adsorption experiments were done as follows. Upon dispersing the desired amount of ACFs in double-distilled water, a given amount of OP stock solution (Pestanal, Sigma Aldrich, Denmark) was added to provide the targeted concentration of adsorbent and pesticide. The vessel containing the mixture of adsorbent (ACF) and given OP was then placed on a laboratory shaker (Orbital Shaker-Incubator ES-20, Grant-bio, UK) at 25 °C for 12 h to ensure

equilibrium conditions (See Supplementary Information, Section S1). The suspension was filtered through a nylon filter (KX Syringe Filter, pore size 220 nm, Kinesis, UK). The concentration of each OP after adsorption in the filtered supernatant (C_{eq}) was determined using ultra performance liquid chromatography (UPLC). Control experiments were performed in identical ways but without ACFs and confirmed no OP degradation during the batch experiments. OP uptake (*UPT*) was used as a measure of the OP removal efficiency and was calculated as:

$$UPT = 100\% \times \frac{C_0 - C_{eq}}{C_0} \quad (1)$$

where C_0 is the starting concentration of OP. Alternatively, the adsorption is quantified as an equilibrium adsorption capacity (q_e), expressed as the mass of adsorbed OP *per* unit mass of adsorbent, given in (mg g^{-1}), calculated as:

$$q_e = 1000 \times \frac{(C_0 - C_{eq}) \times M}{m_{ads}} \quad (2)$$

where M is the molar mass of the pesticide, while m_{ads} is the adsorbent dose (mass concentration). To apply this equation, OP concentration and m_{ads} should be expressed in [mol dm^{-3}] and [g dm^{-3}].

For UPLC measurement, Waters ACQUITY UPLC system with a photodiode array (PDA) detector, controlled by the Empower software, was used. The analyses were done using ACQUITY UPLC™ BEH C18 column (1.7 µm, 100 mm × 2.1 mm, Waters GmbH, GER) under isocratic conditions with a mobile phase A consisting of 10% acetonitrile in water (v/v), and a mobile phase B, which was pure acetonitrile. The eluent flow rate was 0.2 mL min^{-1} in all cases, and the injection volume of 5 µL was used. The composition of the mobile phase and the retention time for dimethoate, malathion, and chlorpyrifos under the given experimental conditions are shown in Table 1. In addition, representative chromatograms and UV–Vis spectra (obtained using PDA detector) of studied OPs are presented in Fig. 1. We note that in this work, we are not interested in OP detection, particularly in mixtures. Thus, we do not use a single multi-residue method for the detection of studied OPs after the adsorption on investigated adsorbents but use the optimal methods for the detection of each studied pesticide.

Toxicity measurements

Modified Ellman's procedure was used to measure the AChE activity of treated water samples (Ellman et al. 1961). The in vitro experiments were performed by exposing 2.5 IU of commercially purified AChE from electric eel to filtered supernatants obtained from batch experiments. This concentration of AChE was found to give an optimal spectrophotometric signal, and it was constant in all experiments. The enzyme and pesticide solution was incubated in a total of 0.650 mL at 37 °C in 50 mM phosphate buffer (pH 8.0). Then, the enzymatic reaction was started by adding acetylcholine-iodide. 5,5′-Dithiobis(2-nitrobenzoic acid) (DTNB) was used as a chromogenic reagent. After 8 min, the reaction was stopped by adding 10% sodium dodecyl sulfate. During the reaction, thiocholine reacts with DTNB and forms colored 5-thio-2-nitrobenzoate, whose absorbance (A) was measured at a wavelength of 412 nm. The toxicity of treated water samples was quantified via the AChE inhibition given as:

$$\text{AChE inhibition}(\%) = 100 \times \frac{A_0 - A}{A_0} \quad (3)$$

where A_0 and A stand for the measured absorbance of the control (no OPs) and the one measured after the exposure to a given OP solution.

Molecular mechanics simulations

Molecular mechanics simulations were done using Avogadro software, with unified force field (UFF) (Hanwell et al. 2012). The carbon surface was generated as a polyaromatic with lateral sizes of roughly 2.7 nm × 2.7 nm, on which oxygen functional groups and phosphorus were introduced. Next, structures of model carbon surface and chlorpyrifos were pre-optimized using molecular dynamics at 300 K, followed by conjugate gradient optimization. All the atoms in the system were allowed to relax fully.

Table 1 Experimental details for UPLC analysis of dimethoate, malathion, and chlorpyrifos. Mobile phase A consists of 10% acetonitrile in water (v/v), while mobile phase B is pure acetonitrile

OP	Mobile phase composition/ v/v%		λ/nm	RT/min	LOD*/mol dm^{-3}
	A	**B**			
Dimethoate	90	10	200	2.375	1×10^{-8}
Malathion	40	60	205	2.482	2×10^{-8}
Chlorpyrifos	20	80	205	2.620	41×10^{-8}

*Limit of detection

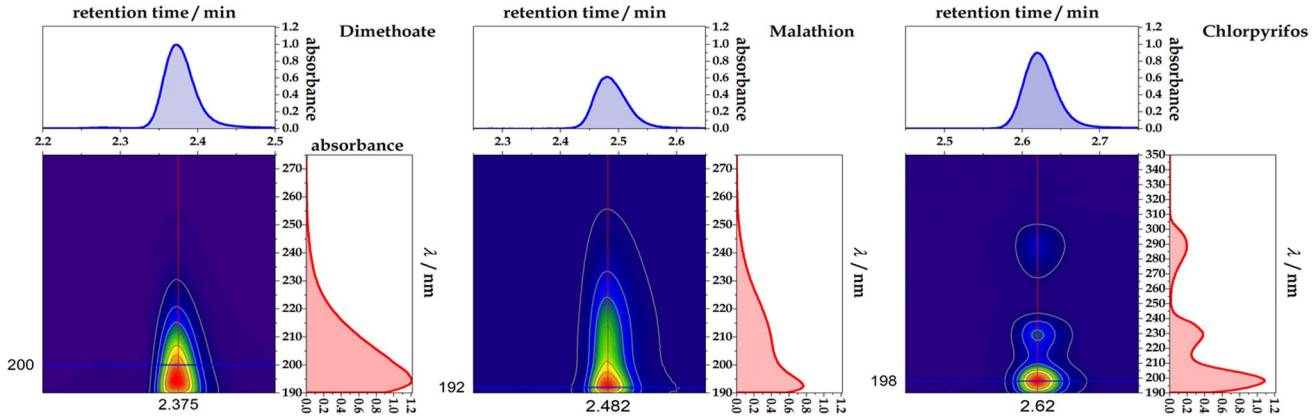

Fig. 1 PDA signals of dimethoate, malathion, and chlorpyrifos, with extracted chromatogram and UV spectra at the retention time, under conditions presented in Table 1 and the common concentration of 5×10^{-4} mol dm^{-3}

Results and discussion

Adsorbents' and OPs' properties

The materials used in this study are described in our recent report (Jocic et al. 2021). The carbon materials are named DAHP-X, where *X* stands for the weight fraction of DAHP used in the impregnation step during the ACF productions ($X=0$ to 10 wt%). For completeness, here we outline and summarize the main characteristic relevant to the present work. Figure 2 shows the correlations between the chemical compositions (obtained using EDX) of studied ACFs regarding carbon, oxygen, and phosphorus content. With the increase of P content, the O content also increases, and there is an excellent correlation between C and O content along the series. However, the P content shows a bit larger scattering. The specific surface area (SSA) and the total pore volume (V_{tot}) increase along with the P content. The increase of V_{tot} (see (Jocic et al. 2021) for pore size distribution curves) follows a relatively good linear trend with certain scattering, but SSA increases more rapidly with the P content, especially at the end of the series where SSAs around 2700 m^2 g^{-1} are reached. More importantly, with the increase of the P content, the mesopore system develops, so materials produced with higher concentrations of DAHP are dominantly mesoporous with large pore volumes (Fig. 2, right).

These materials are rather abundant in terms of O functional groups, including –OH, –C–O–C–, –O–, C–O, and others. These oxygen functionalities incorporated in the carbon lattice bear a partial negative charge and make the studied ACFs hydrophilic. While Raman spectroscopy could not discriminate between these materials, it was unambiguously concluded that a high level of structural disorder characterizes these ACFs.

Structures of studied OPs are given in Fig. 3, along with approximate maximum lateral dimension (measured as a distance between two ends of each molecule) and dipole moment estimated using Avogadro software upon the

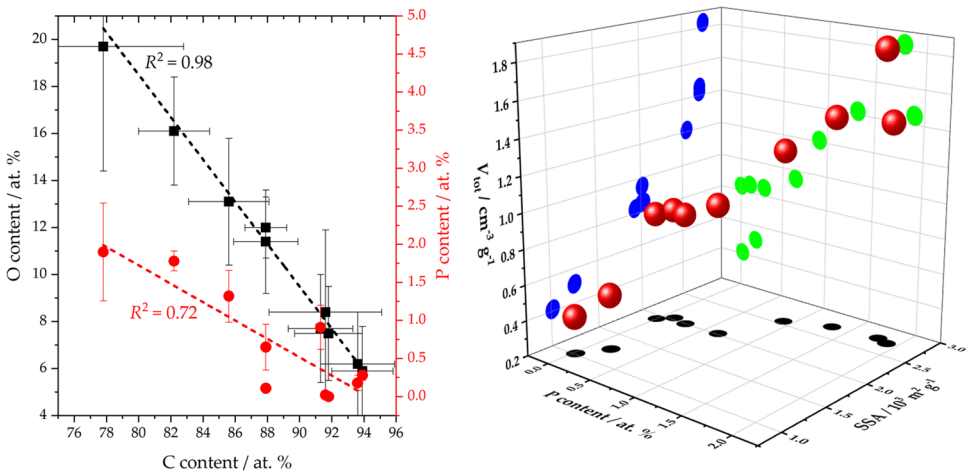

Fig. 2 Left—correlations between C content on one side and P and O content on the other. Right—the 3D plot of the interrelationship between specific surface area, total pore volume, and P content (red spheres); blue, green, and black circles give 2D projections. Data were taken from ref. (Jocic et al. 2021)

structural optimization. While dimethoate and malathion are aliphatic molecules, chlorpyrifos has a Cl-substituted pyridine ring. In all OPs, sulfur from the P = S moiety bears a small positive charge of + 0.003 e, while P is positively charged by 0.23 e. Oxygen atoms bear large negative charges, on average − 0.35 e. The aromatic ring in chlorpyrifos is electron deficient as each Cl atom takes 0.65 e on average, while pyridine nitrogen bears a partial negative charge of − 0.198 e. Estimated values of dipole moment agree well with the solubility of OPs in water. Namely, dimethoate dissolves well in water, while the solubility of malathion is lower (Ozbey and Uygun 2007). The lowest solubility is observed in the case of chlorpyrifos (Ozbey and Uygun 2007). Neurotoxicity follows the opposite trend, and chlorpyrifos has the highest neurotoxicity among considered OPs (Colovic et al. 2013; Lazarević-Pašti et al. 2016).

Adsorption of OPs—screening

We analyzed dimethoate, malathion, and chlorpyrifos adsorption under identical conditions in the first set of experiments. The concentration of ACF adsorbents was 1 mg cm^{-3}, and the concentration of each OP was 5×10^{-4} mol dm^{-3}. Considering the estimated uncertainties of measured uptakes (Fig. 4), the variability among the samples is statistically significant and can be considered the consequence of the different structural and chemical properties of studied ACFs. In general, the lowest uptake was observed for dimethoate. For malathion, very high uptakes were measured (above 99%), where only two samples close to the end of the ACF series showed somewhat lower uptakes (sample DAHP-5 and DAHP-7.5). However, chlorpyrifos was completely removed from the solution (below detection limit of UPLC method used to determine its concentration) for all the samples but DAHP-0.25. For this sample, chlorpyrifos uptake was 99.996%, so the remaining chlorpyrifos concentration in the solution was 2×10^{-8} mol dm^{-3}. We note that this is below the allowed concentration of chlorpyrifos in water (8.6×10^{-8} mol dm^{-3} (Ozbey and Uygun 2007)). We will also show later on that the neurotoxicity is completely alleviated in this case. In order to discriminate between the samples in terms of chlorpyrifos adsorption, we reduced the concentration of adsorbents to 0.1 mg cm^{-3} and the concentration of chlorpyrifos to 1×10^{-4} mol dm^{-3}. Under such conditions, the trends in chlorpyrifos removal can be seen (Fig. 4a). The sample DAHP-0 performs well, but with the introduction of P into the carbon structure, chlorpyrifos removal drops. Then it increases and reaches the maximum for the samples DAHP-1 and DAHP-1.5, after which it begins to decrease.

Due to such efficient chlorpyrifos removal with studied ACFs, we investigated the influence of the OP concentration on the uptake (Fig. 4b). As the concentration of chlorpyrifos decreases, the uptake increases. However, the overall trend in adsorption efficiency is preserved for all the concentrations of chlorpyrifos. The obtained data suggest equilibrium between adsorbed and dissolved chlorpyrifos, indicating no strong chemical bonds formed between the adsorbent surfaces and chlorpyrifos. To put the obtained results in the context of so far reported adsorbents for OP removal, the comparison with the literature data is given in Table 2. Here we focused on the comparison with biomass-derived activated carbons. Clearly, studied materials perform quite well. However, we note that the proper comparison of adsorption capacities would require identical experimental conditions, particularly OP concentration and adsorbent dose, which is almost impossible to find in literature as there are no strict guidelines for performing adsorption measurements.

Removing OPs from their solutions does not necessarily mean that the toxicity of the samples is reduced. Namely, these OPs, if converted to their oxo-analogs, can show

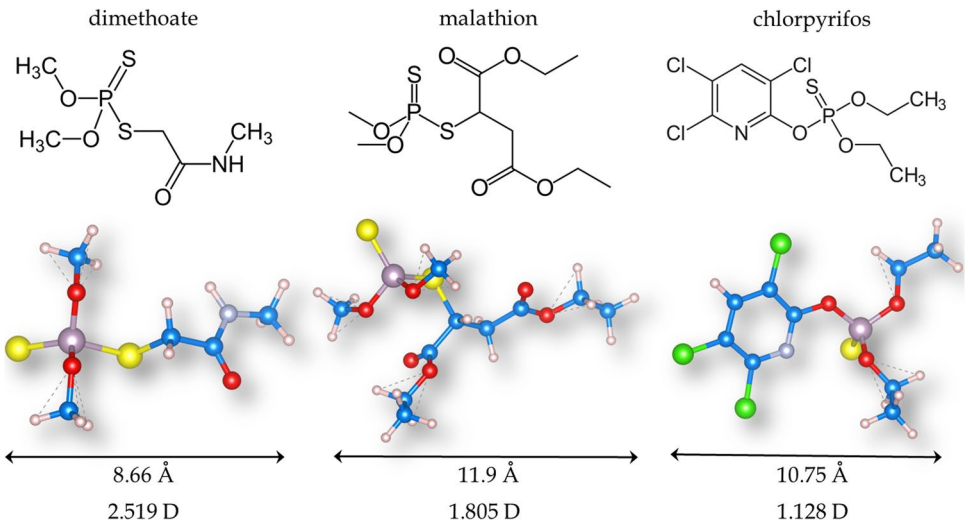

Fig. 3 3D models of investigated pesticides with approximate maximum lateral size of the molecules and dipole moments (in Debye). Color legend: white—hydrogen; blue—carbon; red—oxygen; yellow—sulfur; purple—phosphorus; gray—nitrogen; green—chlorine

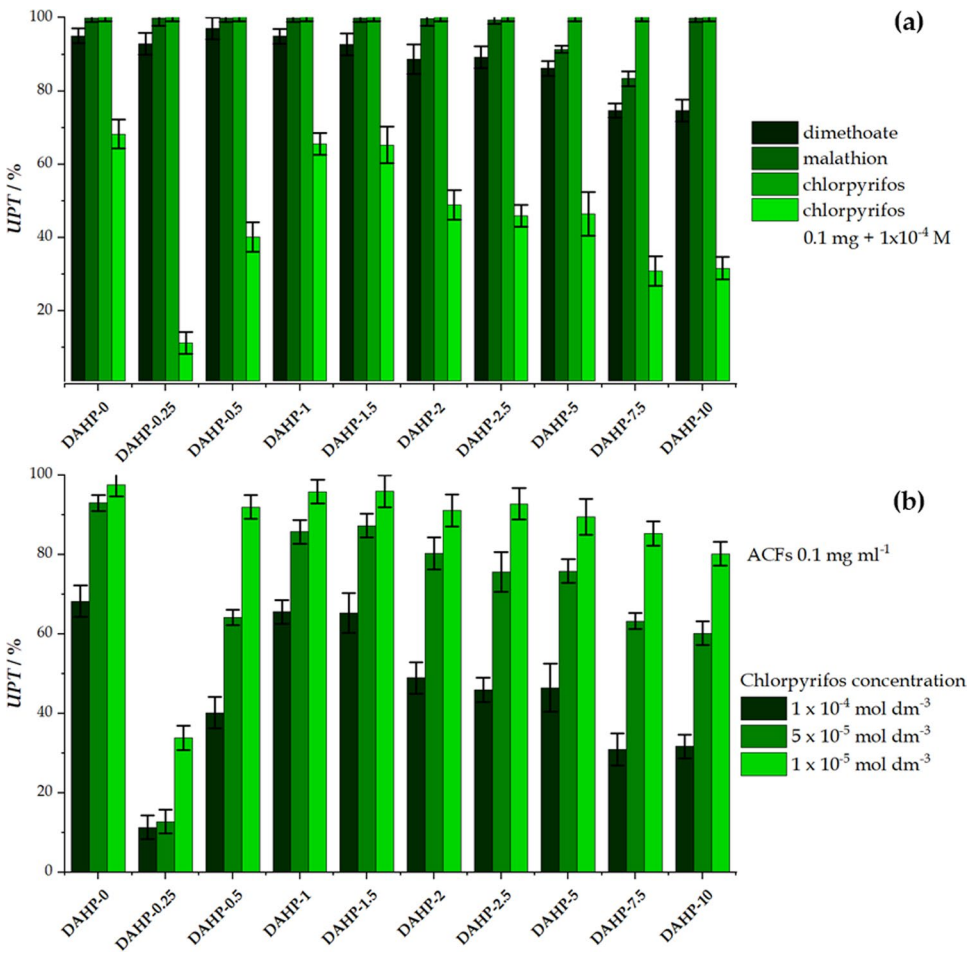

Fig. 4 **a** Measured OPs uptake for 1 mg cm^{-3} ACFs and 5×10^{-4} mol dm^{-3} OPs. For chlorpyrifos, the data for 1×10^{-4} mol dm^{-3} concentration and 0.1 mg cm^{-3} ACFs are also provided; **b** measured chlorpyrifos uptake for three different concentrations and the ACF concentration of 0.1 mg cm^{-3}

up to 1000 higher toxicity (Lazarević-Pašti et al. 2011), so it is important to verify that there is no oxidation of OPs to their more toxic forms during the batch experiments. While such analysis can also be performed using UPLC, the assessment of sample toxicity before and after the OP removal step is an important point that is often disregarded. Namely, the AChE inhibition is a common biomarker for eco-neurotoxicity (Legradi et al. 2018), and

Table 2 Comparison of obtained results with the literature data for dimethoate, malathion, and chlorpyrifos adsorption from aqueous solutions (the results given here are for 1 mg g^{-1} of ACFs and 5×10^{-4} mol dm^{-3} OPs

Pesticide	Adsorbent	Adsorption capacity/mg g^{-1}	Reference
Dimethoate	Activated carbon derived from waste hemp (*Cannabis sativa*) fibers	0.07	(Vukčević et al. 2015)
	KOH modified *Thevetia peruviana* shell activated carbon	70	(Ndifreke and Pasaoglulari Aydinlik 2019)
	DAHP-0.5	111 ± 3	This work
Malathion	Activated carbon from mixed waste	32.1	(Habila et al. 2015)
	Commercial granulated active carbon (GAC)	909.1	(Jusoh et al. 2011)
	Commercially available powdered activated carbon	22	(Kumar et al. 2014)
	DAHP-1.5	165 ± 3	This work
Chlorpyrifos	Activated biochar from tobacco	0.68 to 1.60	(Celso Gonçalves et al. 2021)
	Activated carbon from cinnamon waste	12.4	(Ettish et al. 2021)
	Commercial GAC	173	(Yahia et al. 2021)
	GAC modified with 10 Gy gamma irradiation	273	(Yahia et al. 2021)
	DAHP-0	175 ± 5	This work

we believe that this issue is very important from practical points to identify how proposed adsorbents effectively reduce the toxicity of the contaminated water samples. The absence of oxidation (to levels that would increase toxicity) was confirmed using AChE inhibition tests (Table 3). As can be seen, for the common OP concentration of 5×10^{-4} mol dm^{-3} in spiked tap water, there is appreciable AChE inhibition before the treatment with selected ACFs. The observed trend in the toxicities (dimethoate < malathion < chlorpyrifos) agrees with their toxicity found in the literature (Colovic et al. 2013; Lazarević-Pašti et al. 2016). The best performing materials in the series (Fig. 4a) were used for dimethoate and malathion, and the AChE inhibition was completely removed. However, for chlorpyrifos, the lowest-performing material was used in this test (DAHP-0.25), but, still, AChE inhibition was completely removed upon the adsorption treatment. From these data, we can derive two important conclusions. First, as the measurements were done using spiked water samples, the matrix effects have no appreciable impact on the adsorption performance of studied ACFs for three considered OPs. Second, for all three cases (even for chlorpyrifos for which the remaining concentration is above the allowed one for the used adsorbent), toxicity is completely removed for the OP concentration of 5×10^{-4} mol dm^{-3}. Such a high concentration is almost impossible to find in the environment unless some accident occurred where large concentrations of OPs were released. Hence, acute toxicity can be alleviated using studied ACFs, but one also must consider the negative effects of chronic exposure to OPs at low concentrations (De Silva et al. 2006), as studied ACFs do not remove all the pesticides completely.

Trends in OP adsorption

Previously we showed that multiple linear regression could link material properties to dimethoate uptake (Jocic et al. 2021). Here, we extend this idea and consider jointly three OPs. For dimethoate (Table 4, model 1) and malathion (Table 4, model 2), very good linear regression was obtained using five parameters (C, O, and P content, SSA, and V_{tot}). The R^2 values are 0.9993 in both cases (Table 4; Fig. 5, left). We next focus on chlorpyrifos removal. Using the same five parameters as for dimethoate and malathion, good linear regression models were obtained (Table 4, models CPF1-3; Fig. 5, right) with $R^2 \geq 0.96$. However, after analyzing the goodness of the fit and uncertainties of obtained fitting parameters, we concluded that only three parameters should be sufficient to describe chlorpyrifos removal from water. These are P content (in at.%), SSA (in 10^3 m^2 g^{-1}), and V_{tot} (in cm^3 g^{-1}). Again, good linear regression models were obtained with $R^2 \geq 0.96$ (Table 4, models CPF1.1–3.1; Fig. 5, right). For three different concentrations of chlorpyrifos, one can see a rather constant negative contribution of

Table 3 Results of toxicity measurements. Adsorbent 1 mg cm^{-3}, OPs 5×10^{-4} mol dm^{-3} in tap water, 20 min contact time in batch, 25 °C

	Sample	AChE inhibition before adsorption (% of control)	AChE inhibition after adsorption (% of control)
Dimethoate	DAHP-0.5	35	0
Malathion	DAHP-1.5	89	0
Chlorpyrifos	DAHP-0.25*	95	0

*The lowest-performing material in the series for given experimental conditions

Table 4 The results of multiple linear regression analysis where OP uptake (*UPT*) under different conditions is assumed to be connected to materials properties as $UPT\,(\%) = A\times\text{at.}\%(\text{C}) + B\times\text{at.}\%(\text{O}) + C\times\text{at.}\%(\text{P}) + D\times\text{SSA} + E\times V_{tot}$

	OP concentration/mol dm^{-3}	ACF concentration/g cm^{-3}	*A*	*B*	*C*	*D*/% 10^{-3} g m^{-2}	*E*/% g cm^{-3}	R^2	Model number
Dimethoate	5×10^{-4}	1	0.958	0.588	−6.10	6.00	−10.29	0.9993	1
Malathion			0.975	1.177	5.88	17.07	−40.35	0.9993	2
Chlorpyrifos	1×10^{-4}	0.1	−0.199	−0.252	−35.65	50.18	−13.72	0.96	CPF1
	5×10^{-5}		−0.150	−1.035	−32.22	62.44	−13.44	0.96	CPF2
	1×10^{-5}		0.292	−0.691	−17.08	41.62	−7.87	0.96	CPF3
	1×10^{-4}	0.1			−29.87	37.02	−9.90	0.96	CPF1.1
	5×10^{-5}				−30.77	48.45	−8.86	0.96	CPF2.1
	1×10^{-5}				−29.18	55.77	−11.34	0.97	CPF3.1

P content. As the concentration of chlorpyrifos increases, the contribution of SSA increases, while the contribution of V_{tot} decreases. Obviously, the models are different for different concentrations of adsorbent and chlorpyrifos, but a certain rationalization of observed trends is necessary.

As there is a correlation between the used parameters, one can expect that chlorpyrifos removal efficiency (uptake) will increase as the SSA increases. However, the negative contribution of V_{tot} in all six models for chlorpyrifos uptake suggests that an increase of the pore volume is causing reduced chlorpyrifos uptake. However, in the studied series of ACFs, the increase of V_{tot} is also followed by the increase of pore size (Jocic et al. 2021). Besides, the O content, or in other words, the hydrophilicity of materials surface increases. Therefore, as chlorpyrifos is hardly soluble in water, it can be concluded that it also avoids hydrophilic surfaces so that the maximum of adsorption is reached in the middle of the ACF series using medium DAHP concentrations. This corresponds to increased SSA and V_{tot}, while the O content (indirectly determined by the amount of P in the structure, Fig. 3) is still not too high.

The analysis of chlorpyrifos adsorption on studied ACFs

Considering the extremely high efficiency of studied OPs towards removing chlorpyrifos, we fitted our experimental data into four frequently used adsorption isotherms (Table 5). For all experiments, the ACF concentration was held constant at 0.1 mg g^{-1}. The obtained results are summarized in Tables S2 and S3 (Supplementary Information, Section S2). Raw isotherms are given in Supplementary Information (Figure S1), while linearized forms are given in Fig. 6.

In Table 5, the used parameters are as follows: q_e (mgg^{-1}) equilibrium adsorption capacity, C_e (mg dm^{-3}) equilibrium adsorbate concentration, K_f (mg g^{-1} (mg $dm^{-3})^{1/n}$) and Freundlich constants, q_{max} (mg g^{-1}) theoretical maximum adsorption capacity of the monolayer, b (dm^3 mg^{-1}) Langmuir constant, A_T (dm^3 mg^{-1}) Temkin constant, b_T (kJ mol^{-1}) adsorption heat, q_{DR} maximum adsorption capacity, K_{DR} (mol^2 J^{-2}) constant associated with the mean free adsorption energy *per* mole of adsorbent, E free adsorption energy *per* mole adsorbent $E = (-2K_{DR})^{-1/2}$, $\varepsilon = RT \times \ln(1 + 1/C_e)$. We used linearized forms of isotherms to fit the experimental data, and $R^2$was employed to measure the quality of the fit.

First of all, we see that experimental data fit rather well to all four adsorption isotherms as high values of R^2 were found in practically all the cases. High values of the parameter n in Freundlich isotherm (for $n > 1$, the affinity is considered high) suggest very high affinities of studied ACFs towards chlorpyrifos. While Langmuir isotherm assumes chemisorption and monolayer adsorption on energetically equivalent sites, it provides a rough estimate of the adsorption capacity

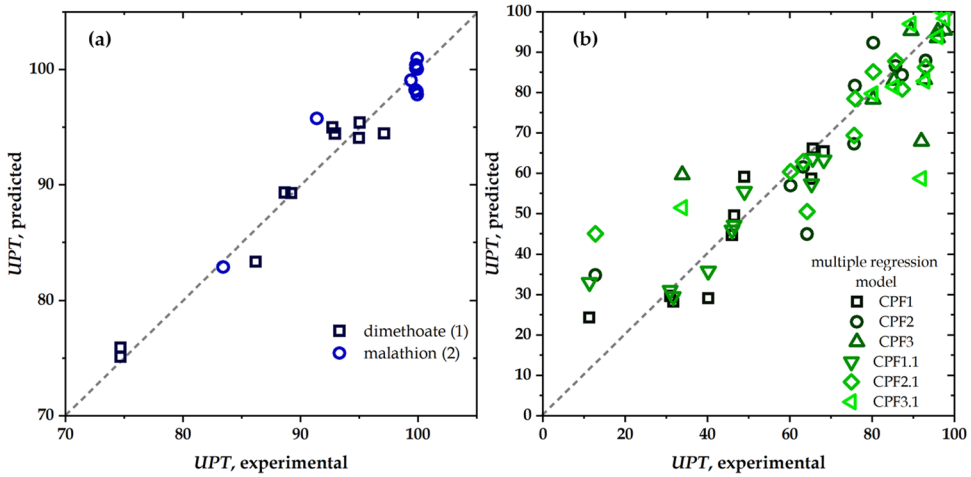

Fig. 5 Parity plot for presented linear regression models: **a** models for dimethoate (1) and malathion (2) uptake, **b** summarized models for chlorpyrifos uptake

Table 5 The equations of used isotherms and their linearized forms(Al-ghouti and Da'ana 2020)

Isotherm	Equation	Linearized form
Freundlich	$q_e = K_f C_e^{1/n}$	$\log q_e = \log K_f + \frac{1}{n}\log C_e$
Langmuir	$q_e = \frac{q_{max} b C_e}{1 + b C_e}$	$\frac{C_e}{q_e} = \frac{1}{b q_{max}} + \frac{C_e}{q_{max}}$
Temkin	$q_e = \frac{RT}{b_T} ln A_T C_e$	$q_e = \frac{RT}{b_T} \ln A_T + \frac{RT}{b_T} \ln C_e$
Dubinin-Radushkevich	$q_e = q_{DR} \exp(-K_{DR}\varepsilon^2)$	$\ln q_e = \ln q_{DR} - K_{DR}\varepsilon^2$

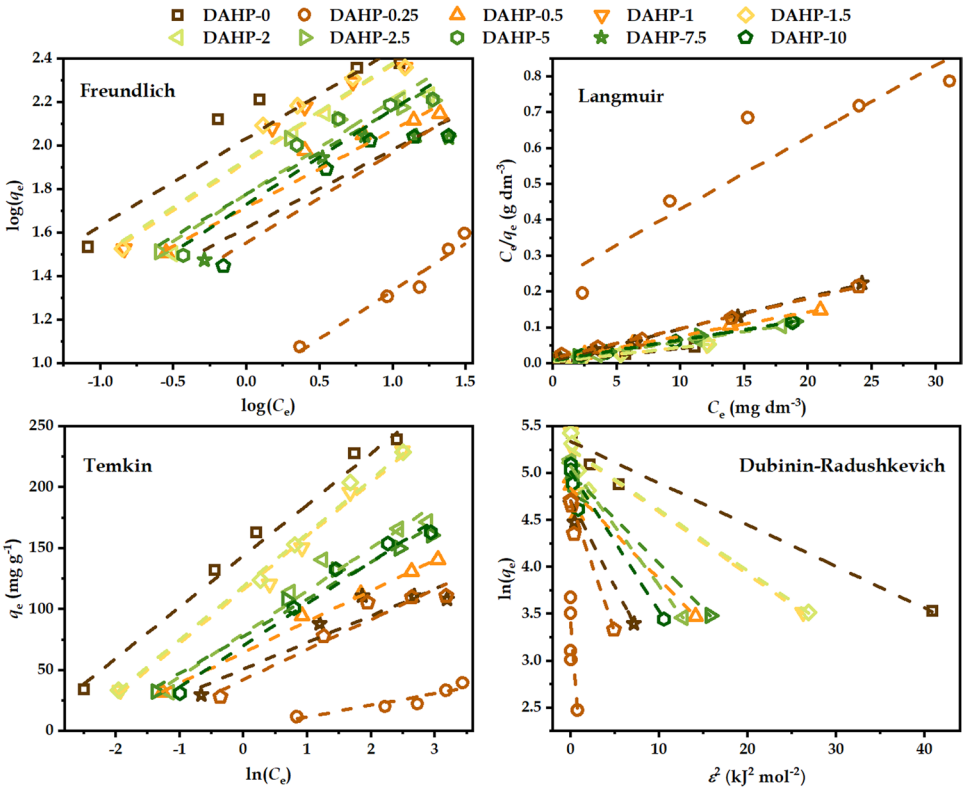

Fig. 6 Fitting experimental data into the linearized forms of four used adsorption isotherms (Freundlich—top left; Langmuir—top right; Temkin—bottom left; and Dubinin-Radushkevich—bottom right)

of studied ACFs under given experiment conditions. These values range between 50 and 250 mg g^{-1}. These values are in accordance with the q_{DR} parameter of the Dubinin-Radushkevich isotherm, although somewhat higher values of q_{max} were obtained using the Langmuir isotherm. However, chemisorption can be excluded in this case. Namely, both Temkin and Dubinin-Radushkevich isotherm predict small heat of adsorption and free adsorption energy, respectively. In the latter case, all the obtained free adsorption energies are below 8 kJ mol^{-1}, indicating physisorption (Silva et al. 2021).

To estimate the theoretical adsorption capacity of studied materials, we have used the lateral dimensions of chlorpyrifos (Fig. 3) and specific surface areas of the studied ACFs. Assuming that chlorpyrifos molecules are hard spheres with diameters matching the determined lateral sizes and that molecules pack densely at ACFs' surface, theoretical capacitances for chlorpyrifos removal are expected to be in the range from 510 to 1387 mg g^{-1} (Table 6). Experimentally obtained values, as well as those predicted using Dubinin-Radushkevich isotherm (q_{DR}), are significantly lower and reach only up to 24.7% of the theoretical capacitance (for DAHP-0). It suggests that only a fraction of the surface is used to adsorb chlorpyrifos. Also, if one disregards the sample DAHP-0.25, the fraction of theoretical adsorption capacity decreases along with the series as the O content (hydrophilicity) increases. This clearly shows that the pore size is not a determinant for chlorpyrifos adsorption. Namely, chlorpyrifos has dimensions of roughly 1 nm (Fig. 3), while the materials at the end of the studied series are largely mesoporous (Jocic et al. 2021). Thus, chlorpyrifos molecules could easily enter the pores. In the entire series of ACFs, the average percentage of theoretical adsorption capacity

Table 6 Measured and theoretical adsorption capacities and the percentage of theoretical adsorption capacity observed experimentally (chlorpyrifos concentration 1×10^{-4} mol dm^{-3} and ACF concentration 0.1 mg cm^{-3})

Sample	Adsorption capacity/mg g^{-1}		
	Experimental (q_{DR})	Theoretical	Percentage of theoretical capacity*
DAHP-0	239 (208.4)	970	24.7
DAHP-0.25	40 (30.4)	510	7.8
DAHP-0.5	141 (126.9)	627	22.5
DAHP-1	230 (190.9)	1022	22.5
DAHP-1.5	229 (193.1)	1005	22.8
DAHP-2	172 (159.8)	1283	13.4
DAHP-2.5	161 (148.3)	1013	15.9
DAHP-5	163 (150.6)	1364	11.9
DAHP-7.5	115 (111.0)	1387	8.3
DAHP-10	111 (110.1)	1364	8.1

*Obtained using experimentally measured adsorption capacity

observed experimentally is 15.8%. If we go back to the assumption that chlorpyrifos molecules are hard spheres, each molecule occupies a 6.3 times larger surface than it covers. Conversely, this means that the distance between chlorpyrifos molecules on the surface is on average 2.5 times the lateral size of the molecule, that is, 2.7 nm. This distance is large enough to exclude adsorbate–adsorbate interactions, partially explaining why Langmuir isotherm gives a good fit to the experimental data (as in the Langmuir model there are no interactions between adsorbate molecules).

To better understand the interactions of chlorpyrifos with the ACF surfaces, molecular mechanics simulations were performed. The standard approach would be using density functional theory (DFT), but DFT is rather demanding for large systems, while the empirical approach is a good choice when the overall trends are investigated. To match the model stoichiometry with the stoichiometry of studied ACFs, a model of the carbon surface with the composition $C_{289}H_{151}O_{32}P$ was constructed. The model consists of a graphene sheet with a lateral dimension of roughly 2.7 nm × 2.7 nm, onto which different functional groups were introduced on the basal plane and edges. Considering the C, O, and P content only, this model consists of 89.75 at. % C, 9.94 at. % O, and 0.31 at. % P. On the other hand, the average chemical composition in the studied series is 88.36 at.% C, 10.8 at.% O, and 0.715 at. % P. The used model includes a region with preserved sp^2 hybridization (Fig. 7, green area), a highly oxidized domain with abundant –OH, –COOH, and –O– groups (Fig. 7, red area), and a P-containing domain around which oxygen functional groups can be found (Fig. 7, a gray area). Such a model setup was based on previous DFT studies, showing that agglomeration of oxygen functional groups occurs on graphene surfaces (Dobrota et al. 2016) and also that point defects and impurities (including phosphorus) serve as attractors for oxygen functional groups on the basal plane (Dobrota et al. 2017). It is noteworthy that the domains with preserved sp^2 hybridization retain planar geometry, while the introduction of P and oxygen functional groups causes the corrugation of the plane.

In the considered carbon surface model, the P atom bears a small negative charge (−0.014 e) while the charge on oxygen atoms is much more negative (−0.5 to −0.3 e). On the other hand, hydrogen atoms from H − C bonds bear a partial positive charge (average 0.04 e), while H atoms from hydroxyl and phenolic groups are more positively charged (0.2 to 0.3 e).

When one chlorpyrifos molecule is added to the system, it covers 15.4% of the surface, closely matching the estimates given in Table 6. Numerous configurations of chlorpyrifos on the model surface were probed, and in all the cases, only weak interactions could be detected, which are supposedly dominated by electrostatic and van der Walls interactions. The interaction energy between the model carbon surface and the chlorpyrifos molecule ranged between −0.15

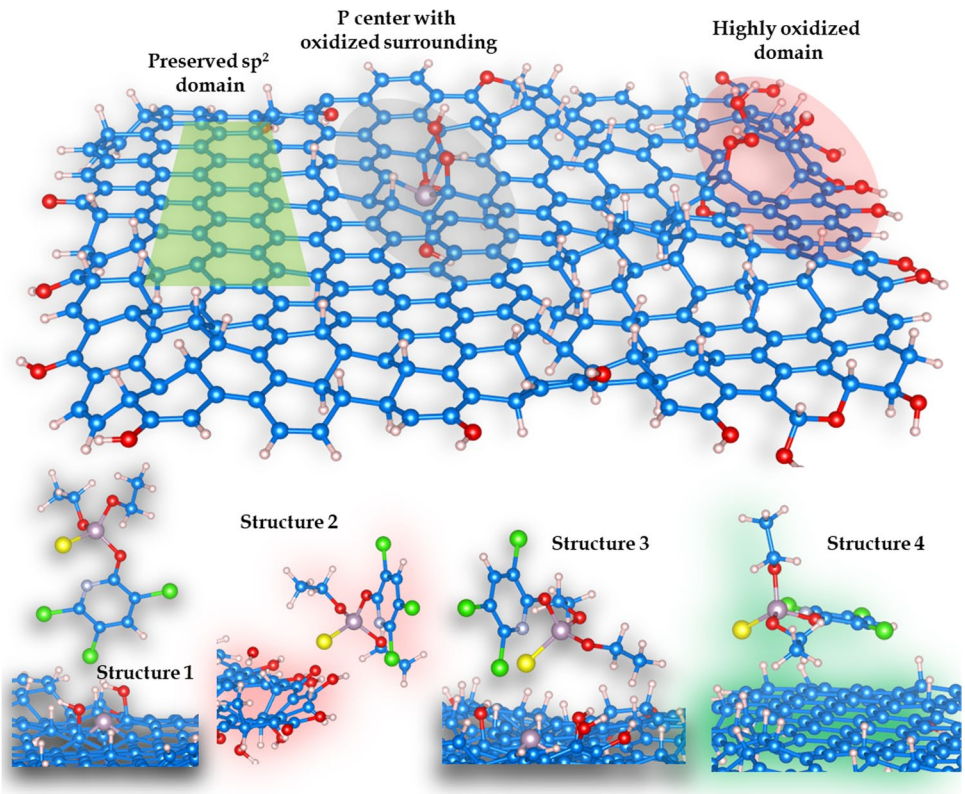

Fig. 7 Optimized structures of model carbon surface with the stoichiometry $C_{289}H_{151}O_{32}P$ (top) and four different configurations of chlorpyrifos interacting with the model surface in different domains (bottom)

and − 0.3 eV. As shown in Fig. 7, several structures present different modes of chlorpyrifos interaction with the surface, with structure 4 being the most favorable in terms of energy. The interaction is achieved via the aromatic ring of chlorpyrifos and the sp^2 hybridized domain of the model carbon surface. Chlorpyrifos is hovering 3.7 Å above the surface, which approximately matches the distance between graphene sheets in graphite of 3.35 Å (Shibuta and Elliott 2011), confirming that weak van der Walls forces govern the interaction. Conversely, this concurs with previous assumptions that hydrophilicity of the surface has a negative effect on chlorpyrifos adsorption. Furthermore, this agrees with the predictions based on the use of Temkin and Dubinin-Radushkevich isotherm regarding dominant physisorption, and it is in harmony with previous findings regarding the interaction of chlorpyrifos with different carbon surfaces (Lazarević-Pašti et al. 2018).

Conclusions

In this contribution, viscose-derived ACFs were screened as adsorbents to remove dimethoate, malathion, and chlorpyrifos from water. Under identical conditions (1 mg cm^{-3} adsorbents and 5×10^{-4} mol dm^{-3}OP), the overall efficiency for OP removal is the highest for chlorpyrifos, followed by malathion and dimethoate. In fact, nine out of ten considered samples completely removed chlorpyrifos from the solution, while the remaining sample had chlorpyrifos uptake above 99.99%. Thus, for all three pesticides, it is possible to find ACFs that completely remove the acute neurotoxicity of solutions even when the initial OP concentrations are as high as 5×10^{-4} mol dm^{-3}. Using regression analysis, studied ACFs' performances towards OP removal were efficiently linked to material properties, specifically their chemical composition and texture. Detailed analysis of chlorpyrifos adsorption on studied ACFs suggests that the physisorption of chlorpyrifos governs the interactions onto hydrophobic parts of the ACFs' surfaces. However, it was concluded that only a small fraction of the surface is operative for chlorpyrifos removal due to the presence of oxygen functional groups and increased hydrophilicity. The maximum adsorption performance is obtained for highly developed surfaces whose hydrophilicity is not high, that is, the ones with lower O and P content. While studied ACFs are eco-friendly and have a great potential for practical application in sustainable water remediation processes, presented results suggest some guidelines for tuning material properties to improve chlorpyrifos uptake even further. Specifically, this relates to the strategic tailoring of carbon surfaces to maximize specific surface areas while reducing oxygen content to increase the contribution of sp^2 hybridized domains for chlorpyrifos adsorption.

Supplementary Information The online version contains supplementary material available at https://doi.org/10.1007/s11356-022-18721-1.

Acknowledgements The authors wish to thank the European Regional Development Fund (EFRE) and the province of Upper Austria for the financial support of this study through the program IWB 2014-2020 (project BioCarb-K). A. J. and T. L. P acknowledge the support provided by the Serbian Ministry of Education, Science, and Technological Development (Contract number: 451-03-9/2021-14/200017). I. A. P. acknowledges the support provided by the Serbian Ministry of Education, Science and Technological Development (Contract number: 451-03-68/2020-14/200146).

Author contribution A. J., S. B., C. U., and C. F. performed experiments and were involved in manuscript preparation; I. P. and T. L. P. were involved in experimental work, supervised all experiments, conceptualized the manuscript, and were major contributors in its writing. All authors read and approved the final manuscript.

Funding This study received financial support from the European Regional Development Fund (EFRE), program IWB 2014–2020 (project BioCarb-K) and the Serbian Ministry of Education, Science and Technological Development (contract numbers: 451–03-9/2021–14/200017 and 451–03-68/2020–14/200146).

Availability of data and materials The datasets used and/or analyzed during the current study are available from the corresponding author on reasonable request.

Declarations

Ethics approval and consent to participate Not applicable.

Consent for Publication Not applicable.

Competing interests The authors declare no competing interests.

References

Al-ghouti MA, Da'ana D (2020) Guidelines for the use and interpretation of adsorption isotherm models : A review. J Hazard Mater 393:122383. https://doi.org/10.1016/j.jhazmat.2020.122383

Breitenbach S, Lumetzberger A, Hobisch MA et al (2020) Supercapacitor electrodes from viscose-based activated carbon fibers: significant yield and performance improvement using diammonium hydrogen phosphate as impregnating agent. C– Carbon Res 6:17. https://doi.org/10.3390/c6020017

Breitenbach S, Unterweger C, Lumetzberger A et al (2021) Viscose-based porous carbon fibers: improving yield and porosity through optimization of the carbonization process by design of experiment. J Porous Mater 28:727–739. https://doi.org/10.1007/s10934-020-01026-4

Celso Gonçalves A, Zimmermann J, Schwantes D et al (2021) Renewable eco-friendly activated biochar from tobacco: kinetic, equilibrium and thermodynamics studies for chlorpyrifos removal. Sep Sci Technol 1–21. https://doi.org/10.1080/01496395.2021.1890776

Colovic MB, Krstic DZ, Lazarevic-Pasti TD et al (2013) Acetylcholinesterase inhibitors: pharmacology and toxicology. Curr Neuropharmacol 11:315–335. https://doi.org/10.2174/1570159x11311030006

Cougnaud A, Faur C, Le Cloirec P (2005) Removal of pesticides from aqueous solution: quantitative relationship between activated carbon characteristics and adsorption properties. Environ Technol 26:857–866. https://doi.org/10.1080/09593332608618497

De Silva HJ, Samarawickrema NA, Wickremasinghe AR (2006) Toxicity due to organophosphorus compounds: what about chronic exposure? Trans R Soc Trop Med Hyg 100:803–806. https://doi.org/10.1016/j.trstmh.2006.05.001

Dehghani MH, Niasar ZS, Mehrnia MR et al (2017) Optimizing the removal of organophosphorus pesticide malathion from water using multi-walled carbon nanotubes. Chem Eng J 310:22–32. https://doi.org/10.1016/j.cej.2016.10.057

Demirbas A (2009) Agricultural based activated carbons for the removal of dyes from aqueous solutions: a review. J Hazard Mater 167:1–9. https://doi.org/10.1016/j.jhazmat.2008.12.114

Dobrota AS, Gutić S, Kalijadis A et al (2016) Stabilization of alkali metal ions interaction with OH-functionalized graphene via clustering of OH groups – implications in charge storage applications. RSC Adv 6:57910–57919. https://doi.org/10.1039/C6RA13509A

Dobrota AS, Pašti IA, Mentus SV, Skorodumova NV (2017) A DFT study of the interplay between dopants and oxygen functional groups over the graphene basal plane – implications in energy-related applications. Phys Chem Chem Phys 19:8530–8540. https://doi.org/10.1039/C7CP00344G

Ellman GL, Courtney KD, Andres V, Featherstone RM (1961) A new and rapid colorimetric determination of acetylcholinesterase activity. Biochem Pharmacol 7:88–95. https://doi.org/10.1016/0006-2952(61)90145-9

Ettish MN, El-Sayyad GS, Elsayed MA, Abuzalat O (2021) Preparation and characterization of new adsorbent from Cinnamon waste by physical activation for removal of Chlorpyrifos. Environ Challenges 5:100208. https://doi.org/10.1016/j.envc.2021.100208

Habila MA, ALOthman ZA, Al-Tamrah SA et al (2015) Activated carbon from waste as an efficient adsorbent for malathion for detection and removal purposes. J Ind Eng Chem 32:336–344. https://doi.org/10.1016/j.jiec.2015.09.009

Hanwell MD, Curtis DE, Lonie DC et al (2012) Avogadro: an advanced semantic chemical editor, visualization, and analysis platform. J Cheminform 4:17. https://doi.org/10.1186/1758-2946-4-17

Hassan MF, Sabri MA, Fazal H et al (2020) Recent trends in activated carbon fibers production from various precursors and applications—a comparative review. J Anal Appl Pyrolysis 145:104715. https://doi.org/10.1016/j.jaap.2019.104715

Jocic A, Breitenbach S, Bajuk-Bogdanović D, et al (2021) Viscose-derived activated carbons fibers as highly efficient adsorbents for dimethoate removal from water. ChemRxiv. doi:https://doi.org/10.33774/chemrxiv-2021-s1dtc This content is a preprint and has not been peer-reviewed.

Jusoh A, Hartini WJH, Ali N, Endut A (2011) Study on the removal of pesticide in agricultural run off by granular activated carbon. Bioresour Technol 102:5312–5318. https://doi.org/10.1016/j.biortech.2010.12.074

Kumar P, Singh H, Kapur M, Mondal MK (2014) Comparative study of malathion removal from aqueous solution by agricultural and commercial adsorbents. J Water Process Eng 3:67–73. https://doi.org/10.1016/j.jwpe.2014.05.010

Lazarević-Pašti T, Anićijević V, Baljozović M et al (2018) The impact of the structure of graphene-based materials on the removal of organophosphorus pesticides from water. Environ Sci Nano 5:1482–1494. https://doi.org/10.1039/c8en00171e

Lazarević-Pašti T, Nastasijević B, Vasić V (2011) Oxidation of chlorpyrifos, azinphos-methyl and phorate by myeloperoxidase. Pestic Biochem Physiol 101:220–226. https://doi.org/10.1016/j.pestbp.2011.09.009

Lazarević-Pašti TD, Pašti IA, Jokić B et al (2016) Heteroatom-doped mesoporous carbons as efficient adsorbents for removal of dimethoate and omethoate from water. RSC Adv 6:62128–62139. https://doi.org/10.1039/c6ra06736k

Legradi JB, Di Paolo C, Kraak MHS et al (2018) An ecotoxicological view on neurotoxicity assessment. Environ Sci Eur 30:1–34. https://doi.org/10.1186/s12302-018-0173-x

Martin-Gullon I, Font R (2001) Dynamic pesticide removal with activated carbon fibers. Water Res 35:516–520. https://doi.org/10.1016/S0043-1354(00)00262-1

Ndifreke WE, Pasaoglulari Aydinlik N (2019) KOH modified Thevetia peruviana shell activated carbon for sorption of dimethoate from aqueous solution. J Environ Sci Heal Part B 54:1–13. https://doi.org/10.1080/03601234.2018.1501143

Ozbey A, Uygun U (2007) Behaviour of some organophosphorus pesticide residues in peppermint tea during the infusion process. Food Chem 104:237–241. https://doi.org/10.1016/j.foodchem.2006.11.034

Shibuta Y, Elliott JA (2011) Interaction between two graphene sheets with a turbostratic orientational relationship. Chem Phys Lett 512:146–150. https://doi.org/10.1016/j.cplett.2011.07.013

Silva MC, Spessato L, Silva TL et al (2021) H3PO4–activated carbon fibers of high surface area from banana tree pseudo-stem fibers: adsorption studies of methylene blue dye in batch and fixed bed systems. J Mol Liq 324. https://doi.org/10.1016/j.molliq.2020.114771

Suo F, Xie G, Zhang J et al (2018) A carbonised sieve-like corn straw cellulose-graphene oxide composite for organophosphorus pesticide removal. RSC Adv 8:7735–7743. https://doi.org/10.1039/c7ra12898c

Uddin S (2021) Removal of pesticides using carbon-based nanocomposite materials. Environmental Remediation Through Carbon Based Nano Composites. Springer, Singapore, pp 365–385

Vukčević M, Kalijadis A, Babić B et al (2013) Influence of different carbon monolith preparation parameters on pesticide adsorption. J Serbian Chem Soc 78:1617–1632. https://doi.org/10.2298/JSC131227006V

Vukčević MM, Kalijadis AM, Vasiljević TM et al (2015) Production of activated carbon derived from waste hemp (Cannabis sativa) fibers and its performance in pesticide adsorption. Microporous Mesoporous Mater 214:156–165. https://doi.org/10.1016/j.micromeso.2015.05.012

Yahia MS, Elzaref AS, Awad MB et al (2021) Efficient adsorption of chlorpyrifos onto modified activated carbon by gamma irradiation; a plausible adsorption mechanism. Zeitschrift Für Phys Chemie 000010151520201765. https://doi.org/10.1515/zpch-2020-1765